Available online at www.sciencedirect.com

SciVerse ScienceDirect

Ceramics International 39 (2013) 3641–3649

CERAMICS INTERNATIONAL

www.elsevier.com/locate/ceramint

Effect of nonstoichiometry on the microstructure and microwave dielectric properties of $Ba(Mg_{1/2}W_{1/2})O_3$ ceramics

Jia Yin Wu, Jian Jiang Bian*

Department of Inorganic Materials, Shanghai University, 149 Yanchang Road, Shanghai, 200072, China

Received 31 July 2012; received in revised form 12 October 2012; accepted 12 October 2012
Available online 23 October 2012

Abstract

Effects of nonstoichiometry on crystal structure and the microstructure of double perovskite $Ba(Mg_{1/2}W_{1/2})O_3$ ceramics have been investigated by X-ray powder diffraction (XRD), scanning electron microscopy (SEM) and Raman spectrometry in this paper. The microwave dielectric properties of the ceramics were studied with a network analyzer at the frequency of about 8–11 GHz. The results show that small deviation from stoichiometric composition has little influence on the crystal structure such as B-site 1:1 ordering degree. Evaporation of BaO was confirmed during the sintering of BMW ceramics, which in turn produce more $BaWO_4$ phase. Ba-deficiency or W-excess in BMW could improve the sinterability and $Q\times f$ value, while Ba-excess or W-deficiency could suppress the formation of $BaWO_4$ at the expense of increase in sintering temperature and decrease in $Q\times f$ value. Mg nonstoichiometry has little effect on the variation of $BaWO_4$ content and $Q\times f$ value. Maximum $Q\times f$ value of about 140,000 GHz could be obtained for the Ba-deficient or W-excessive samples after sintering at 1500 °C/2 h or 1550 °C/2 h, respectively. All Mg-nonstoichiometric compositions exhibit high $Q\times f$ value of about 120,000 GHz after sintering at 1550 °C/2 h. All well-densified samples have dielectric permittivity of about 19–20 and τ_f value varied within the range of $-21\sim-28$ ppm/°C.

Keywords: Double perovskite; Nonstoichiometry; Structure stability; Micowave dielectric properties

1. Introduction

It is well known that high cation ordering leads to large $Q\times f$ values of complex perovskite ceramics. $Ba(Mg_{1/2}W_{1/2})O_3$ (BMW) exhibits the double perovskite structure, in which the B site cations are 1:1 ordered due to their large difference in size and charge. In view of the high ordering degree, BMW is a promising candidate for high-Q dielectric ceramic, which has attracted many attentions [1–5]. Khalyavin et al. have studied the microstructure and microwave dielectric properties of $Ba(Me_{1/2}W_{1/2})O_3$ (Me = Mg, Ni, Zn) [2]. It was found that $Ba(Mg_{1/2}W_{1/2})O_3$ (BMW) double perovskite has dielectric properties of $\varepsilon_r=15$–17.6, $Q\times f=45{,}200-57{,}300$ GHz, $\tau_f=-25$ ppm/°C. $BaWO_4$ impurity phase appears at temperature >1200 °C. Above its melting point of about 1475 °C [6], liquid phase is formed and remains at triple grained boundary junction as a sintering additive. Microwave dielectric properties of $\varepsilon_r=8.1$, $Q\times f=57{,}500$ (GHz), $\tau_f=-78$ ppm/°C has been reported for $BaWO_4$ by Yoon et al. [7]. Bian et al. [4] investigated the microwave dielectric properties of $A_{1-3x/2}La_x(Mg_{1/2}W_{1/2})O_3$ (A = Ba, Sr, Ca; $0.0\leq x\leq0.05$), and found that small amount of La-substitution for A site cation could suppress the formation of AWO4 at high temperature. Small level of La-substitution for Ba ($x=0.02$) substantially improves the $Q\times f$ value to more than 100,000 GHz, however increases the sintering temperature to about 1600 °C simultaneously due to the lack of $BaWO_4$ liquid phase. In our previous paper [5], we studied the structure stability and microwave dielectric properties of Ca-doped BMW ($Ba_2Mg_{1-x}Ca_xWO_6$). The structure instability and decomposition of Ba_2MgWO_6 at high temperature are suggested to be caused by the large lattice strain energy due to the under-bonded Mg–O and over-bonded Ba–O bonds. This view is supposed be generalized to the instability of other complex perovskites such as $Ba(Zn_{1/3}W_{1/2})O_3$, $Ba(Zn_{1/3}Nb_{2/3})O_3$ and $Ba(Mg_{1/3}Ta_{2/3})O_3$, in which barium

---

*Corresponding author. Fax: +86 21 56331697.
E-mail address: jjbian@shu.edu.cn (J. Jiang Bian).

http://dx.doi.org/10.1016/j.ceramint.2012.10.193

tungstate, barium niobate and barium tantalate could be easily formed at high temperature, respectively. Small amount of Ca-doping is also useful to the suppression of $BaWO_4$ formation due to the increase in Mg/Ca–O bond strength and decrease in Ba–O bond strength. However it still cannot completely suppress the decomposition of $Ba_2Mg_{1-x}Ca_xWO_6$ at the sintering temperature above 1400 °C. Excellent combined microwave dielectric properties with $\varepsilon_r = 20.8$, $Q \times f = 120{,}729$ GHz, and $\tau_f = 0$ ppm/°C could be obtained by small level of Ca-doping ($x = 0.1$). However the remained amorphous MgO and BaO, which accompanied with the appearnce of $BaWO_4$ in BMW ceramic, considerably decrease the $Q \times f$ value when the sample was stored under ambient conditions for a long time due to the hygroscopy of MgO and BaO in the air humidity [5]. Complete suppression of the decomposition of BMW during sintering is therefore of crucial importance for practical application.

The decomposition of Ba_2ZnWO_6 at high temperature is confirmed to be caused by the sublimation of ZnO due to its high partial pressure in air [8]. However, in the case of Ba_2MgWO_6, the vaporization of BaO rather than MgO should be expected due to its comparatively high vapor pressure at high temperature [9]. The possible vaporization of BaO would in turn facilitate the decomposition of Ba_2MgWO_6 and shift the bulk composition chemistries toward the WO_3-richer portion of the system, which would produce more secondary phases including $BaWO_4$ and MgO according to the mass balance equation. Therefore excessive BaO content is supposed to hinder the appearance of $BaWO_4$. For many barium based complex preovskites such as $Ba(Mg_{1/3}Ta_{2/3})O_3$, $BaZn_{1/3}Nb_{2/3}O_3$, it is has been reported that small deviations from its stoichiometric composition have pronounced effects on the phase constituent, sinterability, B-site cations ordering and microwave dielectric properties [10–13]. On the whole, small amount of A-site or B′-site deficiency around the stoichiometric composition usually improves the sinterability and ordering degree of B site cations, hence considerably increases the microwave quality factor. But over deficiency of A-site cation would result in the appearance of impurity phases such as barium niobates or barium tantalates, which leads to the decrease in $Q \times f$ value. Opposite effect is observed for the A-site or B′-site excessive compositions.

In this paper, therefore, we have investigated the effect of A, B′ and B″ site cation nonstoichiometry on the phase composition, microstructure and microwave dielectric properties of BMW.

2. Experimental

The samples of $Ba_{1+x}(MgW)_{1/2}O_3$ ($x = -0.015$, -0.010, -0.005, 0, 0.005, 0.010 and 0.015), $Ba(Mg_{1+y}W)_{1/2}O_3$ ($y = -0.02$, -0.01, 0, 0.01 and 0.02) and $Ba(MgW_{1+z})_{1/2}O_3$ ($z = -0.02$, -0.01, 0, 0.01 and 0.02) were prepared by a conventional solid-state reaction process from $BaCO_3$ (99.7%), MgO(99.7%), and WO_3(99.5%) starting materials. The starting materials were weighed according to the above formula and ball milled in ethanol with zirconia milling media for 24 h, then dried and calcined at 1200 °C for 2 h in

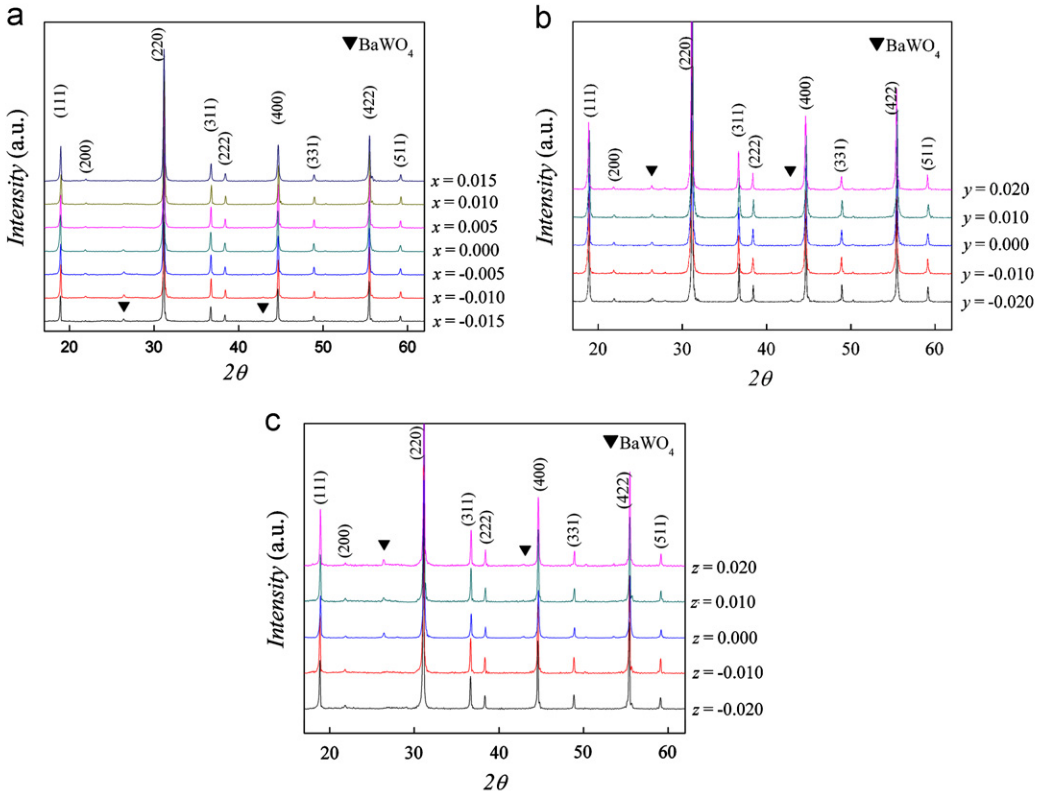

Fig. 1. Powder XRD patterns for (a) $Ba_{1+x}(MgW)_{1/2}O_3$, (b) $Ba(Mg_{1+y}W)_{1/2}O_3$ and (c) $Ba(MgW_{1+z})_{1/2}O_3$ sintered at 1500 °C/2 h.

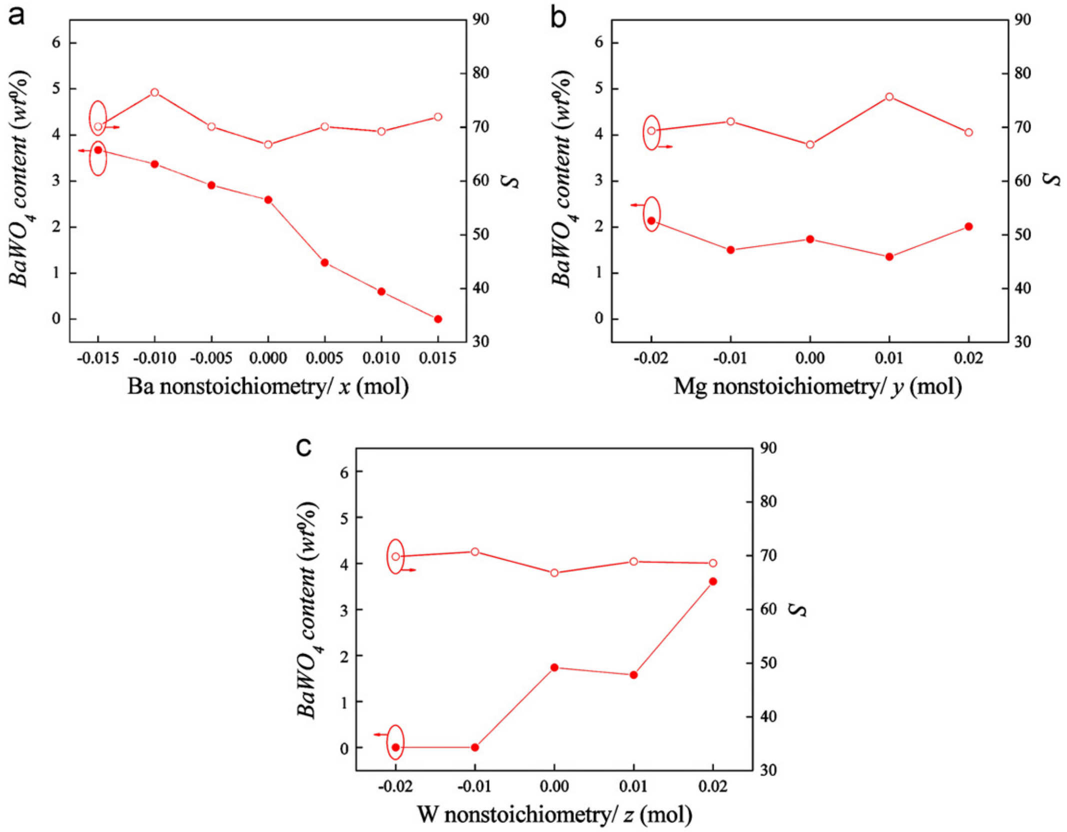

Fig. 2. Variations of $BaWO_4$ content and ordering degree with nonstoichiometry for (a) $Ba_{1+x}(MgW)_{1/2}O_3$, (b) $Ba(Mg_{1+y}W)_{1/2}O_3$ and (c) $Ba(MgW_{1+z})_{1/2}O_3$, respectively.

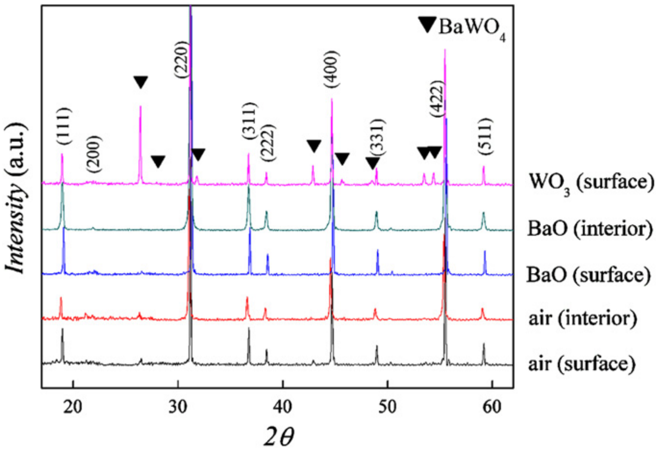

Fig. 3. XRD patterns from the surface and interior of $Ba(Mg_{1/2}W_{1/2})O_3$ sintered at 1500 °C/2 h in different atmosphere.

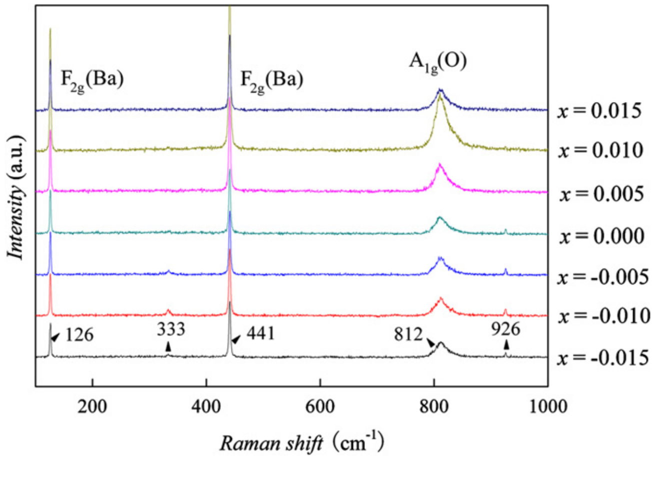

Fig. 4. Raman spectra of barium-nonstoichiometric $Ba(Mg_{1/2}W_{1/2})O_3$ ceramics sintered at 1500 °C/2 h.

alumina crucible. The calcined powders were pulverized again by ball milling in ethanol for 24 h. After drying, mixed with 7–10 wt% PVA and sieving, the granulated powders were uniaxially pressed into compacts 10 mm in diameter and 4.5 mm thickness under a pressure of 120 MPa. The compacts were sintered at 1450–1600 °C for 2 h in ambient atmosphere. In addition, to further clarify the formation of $BaWO_4$, a BaO or WO_3-rich atmosphere was maintained during the sintering of the stoichiometric composition pellets by placing $BaCO_3$ or WO_3 powder around the pellets inside the covered alumina crucible.

The phase constituents of the sintered samples were identified by X-ray diffraction (XRD) with Ni-filtered Cu Kα radiation (Rigaku D\max 2200, Japan). The $BaWO_4$ content were estimated via Jade 5.0 software. The Raman experiments were carried out for the sintered samples

(RENIShaw in Via plus, UK). The Raman spectra were excited with the 785 nm line of a semiconductor laser at a power of 250 mW and recorded in back-scattering geometry using InVia Raman Microscope equipped with a grating filter, enabling good stray light rejection in the 100–1000 cm range. The microstructure of the sintered sample was characterized by scanning electron microscopy (SEM) (HITACHI SU-1500, Japan). The samples were polished and thermally etched at the temperature of 150 °C lower than its sintering temperature for 30 min. The densities of the ceramics were measured by the Archimedes method. Microwave dielectric properties of the sintered samples were measured between 7 GHz and 13 GHz using a network analyzer (Agilent N5230A, USA). The quality factor was measured by the transmission cavity method. The dielectric permittivity (ε_r) was measured according to the Hakki–Coleman method using the TE_{011} resonant mode, and the temperature coefficient of the resonator frequency (τ_f) was measured using invar cavity in the temperature range from 20 °C to 80 °C.

3. Results and discussion

The powder X-ray diffraction patterns for barium-, magnesium- and tungsten-nonstoichiometric BMW sintered at 1500 °C/2 h in air are shown in Fig. 1. All the compounds are easily identified to adopt the cubic perovskite structure and can be indexed in the space group of *Fm–3m*. Small amount of impurity $BaWO_4$ phase could be detected in $Ba_{1+x}(MgW)_{1/2}O_3$ ($x \leq 0.01$), $Ba(Mg_{1+y}W)_{1/2}O_3$ ($-0.02 \leq y \leq 0.02$) and $Ba(MgW_{1+z})_{1/2}O_3$ ($z \geq 0$) compositions. BaO and MgO-rich phase(s) are expected to present according to the mass balance equation ($Ba_2MgWO_6 \rightarrow BaWO_4 + BaO + MgO$). However no BaO and MgO-rich phase(s) could be detected by XRD as reported before [7]. The reflections of the MgO-rich phase are probably lost in the background and the BaO-rich phase might be in the amorphous state like in the case of Ba_2ZnWO_6 ceramic [8]. Variations of $BaWO_4$ content with barium-, magnesium- and tungsten-nonstoichiometry are shown in Fig. 2(a)–(c) respectively. A comparison of Fig. 2 reveals that Ba-excess or W-deficiency suppresses the formation of $BaWO_4$ phase as expected. Whereas Mg nonstoichiometry (y) seems to have little effect on the variation of $BaWO_4$ content. It indicates that the evaporation of BaO is responsible for the increase of $BaWO_4$ phase. The activity of BaO is expected to increase with the increase of its excessive amount because of its high vapor pressure at the sintering temperature, which suppresses the formation of $BaWO_4$ phase according to the mass balance equation. In contrast, the activity of MgO changes little regardless of the excessive amount due to its low vapor pressure at the sintering temperature. This may explain the reason why Mg nonstoichiometry (y) has little effect on the variation of $BaWO_4$ content. W-deficiency is essentially equivalent to Ba- and Mg-excess, thus has similar effect. Excessive WO_3 would more likely react with the remained BaO than MgO to produce $BaWO_4$ instead of $MgWO_4$ because of the larger enthalpy of $BaWO_4$ compared with that of $MgWO_4$ [14]. So the $BaWO_4$ amount increases with the increase of the excessive amount of WO_3, as shown in Fig. 2(c). The XRD patterns from the surface of stoichiometric composition sintered at 1500 °C/2 h in BaO or WO_3 vapor as shown in Fig. 3 are in well agreement with those of Ba- or W-excessive compositions. The XRD pattern from the interior of

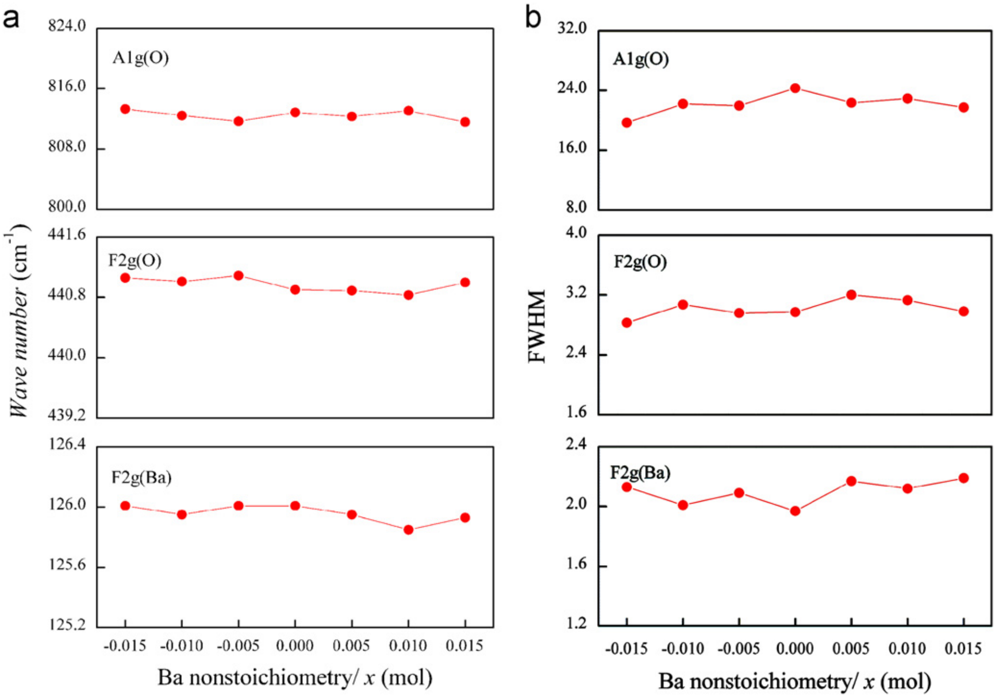

Fig. 5. Variations of mode frequency and FWHM for the three main modes in $Ba_{1+x}(MgW)_{1/2}O_3$.

the sectioned stoichiometric BMW sample sintered at 1500 °C/2 h in BaO vapor also demonstrates no $BaWO_4$ phase. Whereas that from the interior of the sectioned sample sintered at 1500 °C/2 h in air still shows the presence of $BaWO_4$ phase (Fig. 3). It seems to indicate that the evaporation of BaO is not limited to the surface area. The formation of $BaWO_4$ coupled with BaO and MgO from the thermal decomposition of Ba_2MgWO_6 is caused by the presence of large lattice strain energy due to the under-bonded Mg–O and over-bonded Ba–O bonds. The vaporization of BaO in turn facilitates the decomposition of Ba_2MgWO_6 and shift bulk composition chemistries toward the WO_3-richer portion of the system, which would produce more secondary phases including $BaWO_4$ and MgO according to the mass balance equation.

The noticeable intensity of (111) reflection indicates high ordering of the B-site cations. The ordering degree of 1:1 B-site cation estimated by $S=(I_{111}/I_{200})_{obs}/(I_{111}/I_{200})_{calc}$ [15] is also shown in Fig. 2. As can be seen, small deviations of Ba, Mg or W from stoichiometry of BMW have little effect on the B-site ordering degree, which varies slightly around 70% for all compositions.

Raman spectroscopy is considered to be an ideal tool for probing the local crystal structure. Fig. 4 presents the Raman spectra of barium-nonstoichiometric BMW ceramics sintered at 1500 °C/2 h. The Mg- or W-nonstoichiometric compositions exhibit very similar Raman spectra as those shown in Fig. 4 (not shown here). All compositions show three main Raman-active modes including $A_{1g}(O)$ at 812 cm^{-1}, $F_{2g}(O)$ at 441 cm^{-1} and $F_{2g}(Ba)$ at 126 cm^{-1}, which is consistent with the observations for other 1:1 ordered perovskites. The expected $E_g(O)$ mode is too weak to be detected here. The two weak bands at 333 cm^{-1} and 926 cm^{-1} appeared in the Ba-deficient compositions resulted from the $BaWO_4$ impurity phase. No first order Raman active mode is expected for MgO phase due to its center symmetry. Also no Raman active modes from BaO is observed probably due to its amorphous state, which is in agreement with the XRD data. The decrease in FWHM of $A_{1g}(O)$ is usually used to indicate an increase in 1:1 ordering. However, the little changed mode frequency and line width (FWHM) for the three main modes (Fig. 5) indicates no obvious crystal structural evolution with small nonstoichiometry of BMW. This is inconsistent with those reported for $Ba(Mg_{1/3}Ta_{2/3})O_3$ and $BaZn_{1/3}Nb_{2/3}O_3$ in which cases small amount of Ba-deficiency usually increases its 1:2 ordering. The reason may be related to the larger charge difference between B-site cations in BMW than that in $Ba(Mg_{1/3}Ta_{2/3})O_3$ or $BaZn_{1/3}Nb_{2/3}O_3$.

Fig. 6 shows the SEM images of the nonstoichiometric BMW samples sintered at 1500 °C/2 h. The Ba-deficient or W-excessive specimens demonstrate well-developed microstructures with large average grain size. In contrast the ceramics with small amount of Ba-excess or W-deficiency exhibit small grain size and poor densification. The improvement of sinterability for the specimens with small amount of Ba-deficiency or W-excess can be attributed to the appearance of $BaWO_4$ liquid phase during sintering (Fig. 1). From the nearly spherical shape of the grain surface regions exposed at the triple junctions, the solid–liquid interfacial energy of this system is expected to more or less isotropic. In contrast, the poor sinterability for the Ba-excessive or W-deficient specimens can be ascribed to the disappearance of $BaWO_4$ liquid phase (Fig. 1) and the possible presence of excessive amorphous BaO phase which remained at grain boundaries and hindered the grain boundary migration. The BaO phase is hardly recognizable by SEM and XRD, which is in agreement with those observed for other Ba-excessive complex perovskites [10,11]. Notice that the trend of decrease in density and grain size with the increase in barium-excessive amount is reversed at $x=0.015$ composition. The round surface of the grain seems to infer the forming of another barium containing liquid phase in the barium over excessive composition ($x=0.015$), which is hardly recognizable by SEM and XRD analysis probably due to its trace amount. The microstructure changes little for the Mg-nonstoichiometric compositions. All samples demonstrate dense microstructure due to

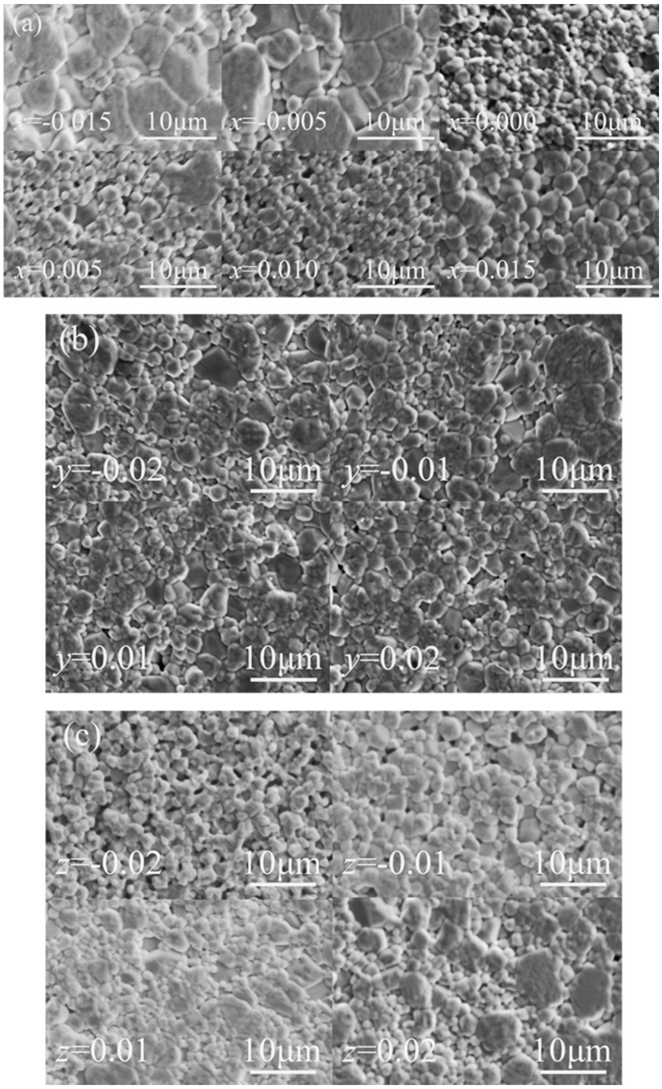

Fig. 6. SEM images of (a) $Ba_{1+x}(MgW)_{1/2}O_3$, (b) $Ba(Mg_{1+y}W)_{1/2}O_3$ and (c) $Ba(MgW_{1+z})_{1/2}O_3$ ceramics sintered at 1500 °C/2 h.

the liquid phase sintering by $BaWO_4$. No MgO phase could be observed in the SEM images for all compositions, even in the Mg-excessive compositions, which is not in agreement with our former report that amorphous MgO-rich phase crystallized during the thermal etching process at 1400 °C/30 min[5]. The reason can be explained by the lower thermal etching temperature adopted in this case (1350 °C/30 min).

Variations of relative density for $Ba_{1+x}(MgW)_{1/2}O_3$, $Ba(Mg_{1+y}W)_{1/2}O_3$ and $Ba(MgW_{1+z})_{1/2}O_3$ ceramics sintered at different temperatures as function of x, y and z respectively are shown in Fig. 7. The density variation with nonstoichiometry is well consistent with the corresponding change of microstructure observed by SEM. The Ba-deficient or W-excessive samples are well sintered and reach optimized relative densities above 96% TD. The density decreases and sintering temperature increases with the increase of barium-excessive or tungsten-deficient amount. Also noted that the relative density for barium-excessive composition with $x=0.015$ is larger compared with that of $x=0.01$ composition. The density changes little for the Mg-nonstoichiometric compositions. All samples could be densified to about 96% TD after sintering at 1500 °C/2 h.

Fig. 8 shows the variations of dielectric permittivity with nonstoichiometry for BMW sintered at different temperatures. The variation of dielectric permittivity with nonstoichiometry exhibits the same varying trend as that of density for the samples sintered at 1450–1550 °C/2 h. It means that the dielectric permittivity of the sample is mainly influenced by the corresponding relative density, and generally increases with the increase of density. The influence of impurity phases on the dielectric permittivities in this case can be neglected due to their trace amounts. All well-densified samples demonstrate dielectric permittivity of about 19–20. However, for the Mg-nonstoichiometric compositions sintered at 1600 °C/2 h, the decrease in dielectric permittivity can be ascribed to the increase of $BaWO_4$ content, which has lower ε_r compared with that of BMW, with the further increase of sintering temperature.

Fig. 9. shows the variations of the $Q\times f$ value for $Ba_{1+x}(MgW)_{1/2}O_3$, $Ba(Mg_{1+y}W)_{1/2}O_3$ and $Ba(MgW_{1+z})_{1/2}O_3$ ceramics sintered at different temperatures. The $Q\times f$ value varies with the sintering temperature for the fixed composition. The optimized $Q\times f$ values of the Ba-deficient or W-excessive samples are much larger than those of Ba-excessive or W-deficient samples. Maximum $Q\times f$ value of about 140,000 GHz could be obtained for the Ba-deficient or W-excessive samples after sintering at 1500 °C/2 h or 1550 °C/2 h, respectively. The $Q\times f$ value changes little for the Mg-nonstoichiometric compositions. All samples exhibit

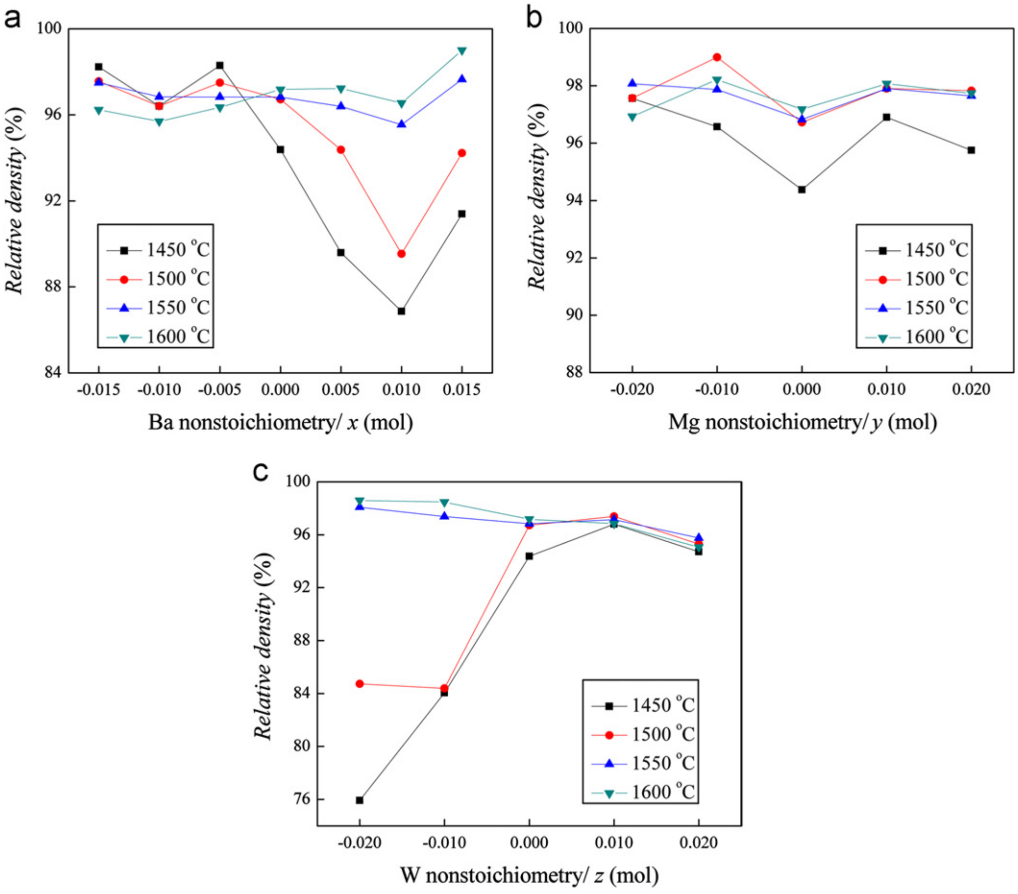

Fig. 7. Variation of density with nonstoichiometry for (a) $Ba_{1+x}(MgW)_{1/2}O_3$, (b) $Ba(Mg_{1+y}W)_{1/2}O_3$ and (c) $Ba(MgW_{1+z})_{1/2}O_3$ ceramics sintered at different temperatures.

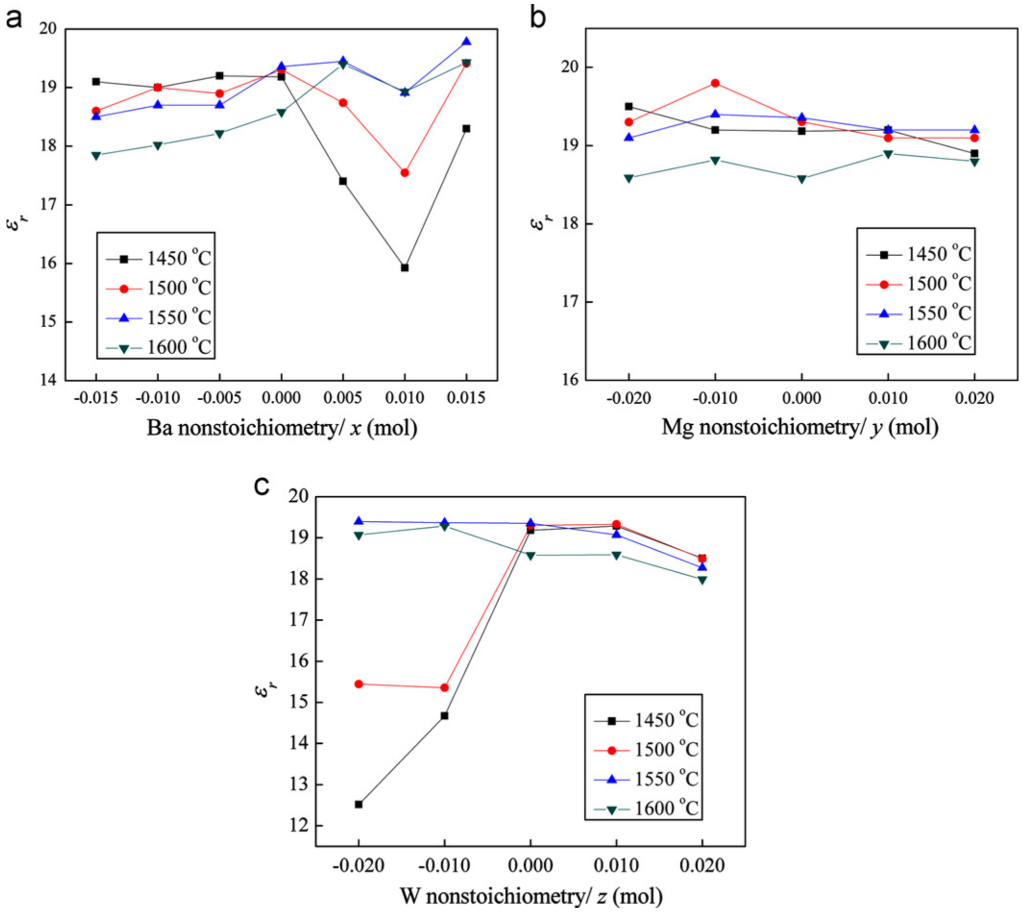

Fig. 8. Variation of dielectric permittivity with nonstoichiometry for (a) $Ba_{1+x}(MgW)_{1/2}O_3$, (b) $Ba(Mg_{1+y}W)_{1/2}O_3$ and (c) $Ba(MgW_{1+z})_{1/2}O_3$ ceramics sintered at different temperatures.

high $Q\times f$ value of about 120,000 GHz after sintering at 1550 °C/2 h. It is well known that microwave dielectric losses are contributed by both intrinsic and extrinsic losses. The former is related to the crystal structure such as order–disorder, while the latter is related to the microstructure (e.g. pores, boundaries and second phases). Since crystal structure such as B-site 1:1 ordering degree changed little with the nonstoichiometry as discussed above, the considerable change of $Q\times f$ value for the Ba- or W-nonstoichiometric composition is supposed to be attributed to the extrinsic factors such as density and impurity phases. The remarkable decrease in $Q\times f$ value for the Ba-excessive or W-deficient samples sintered below 1550 °C/2 h can be ascribed to the decrease in density and increase in remained BaO lossy phase. For those well densified barium-excessive or tungsten-deficient samples sintered at 1550 °C/2 h, the effect of porosity on the $Q\times f$ value could be neglected. So, the sharp decrease in $Q\times f$ value is mainly caused by the increase in excessive BaO lossy phase. And the improvement of $Q\times f$ value for the Ba-deficient or W-excessive samples is mainly benefited from the decrease in BaO impurity lossy phase and increase in density by the liquid phase sintering of $BaWO_4$. Since $BaWO_4$ and MgO are reported to have comparatively high $Q\times f$ value [7,16], so the presences of trace amount of $BaWO_4$ and MgO phases have little effect on the total $Q\times f$ value of the system. However, the presence of remained MgO and BaO phase in the sample would deteriorate the $Q\times f$ value after it was stored under ambient conditions for a long time because of the hygroscopy of MgO and BaO in the air humidity. The $Q\times f$ value could be restored to its former level after the sample was heat-treated again at 1200 °C/2 h due to the dehydration. The temperature coefficient of resonator frequency (τ_f) changes slightly with the nonstoichiometry. The τ_f values for all compositions are within the range of -21–-28 ppm/°C (Fig. 10). The τ_f value of pure $BaWO_4$ is about -78 ppm/°C. Although the content of $BaWO_4$ changed almost linearly with the x and z value as shown in Fig. 2(a) and (c). However the τ_f values of nonstoichiometric $Ba(Mg_{1/2}W_{1/2})O_3$ did not show the similar trends. This can be explained by the presence of MgO and possible remained BaO amorphous phases in addition to $BaWO_4$ as discussed above, which also affected the τ_f values.

4. Conclusions

The influences of Ba-, Mg- and W-nonstoichiometry on the phase composition, microstructure, and microwave dielectric properties of double perovskite $Ba(Mg_{1/2}W_{1/2})O_3$

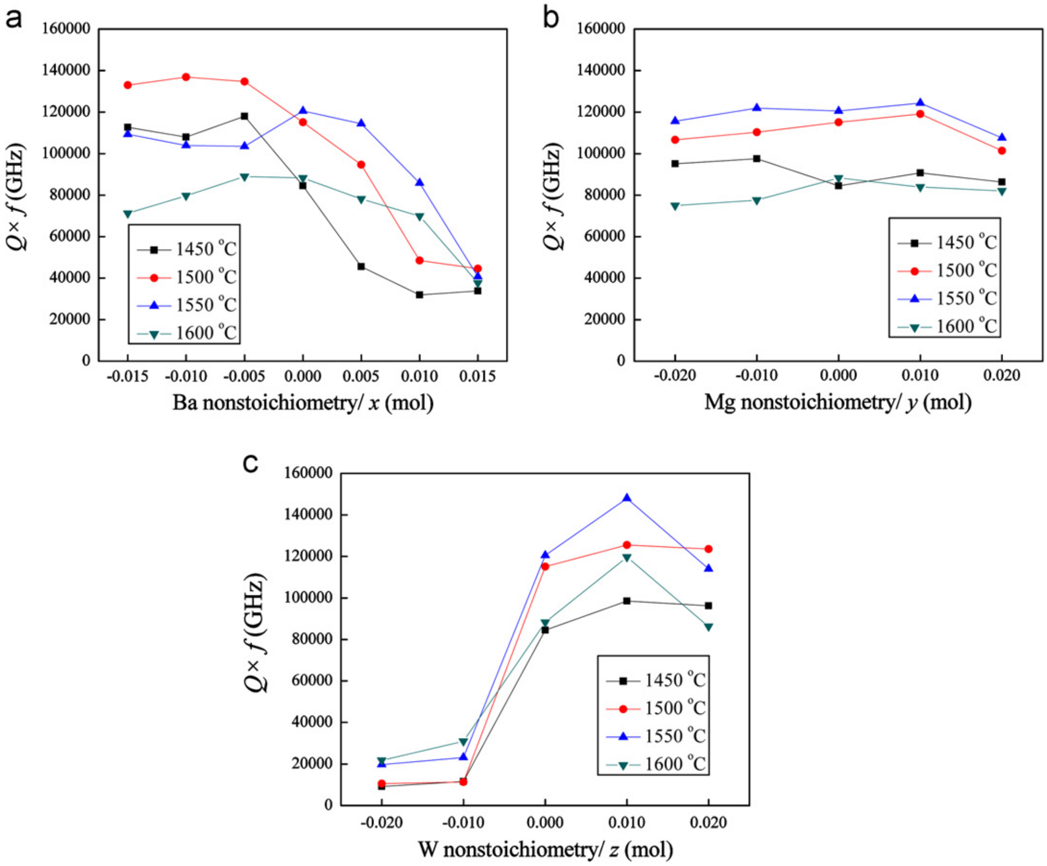

Fig. 9. Variation of $Q \times f$ value with nonstoichiometry for (a) $Ba_{1+x}(MgW)_{1/2}O_3$, (b) $Ba(Mg_{1+y}W)_{1/2}O_3$ and (c) $Ba(MgW_{1+z})_{1/2}O_3$ ceramics sintered at different temperatures.

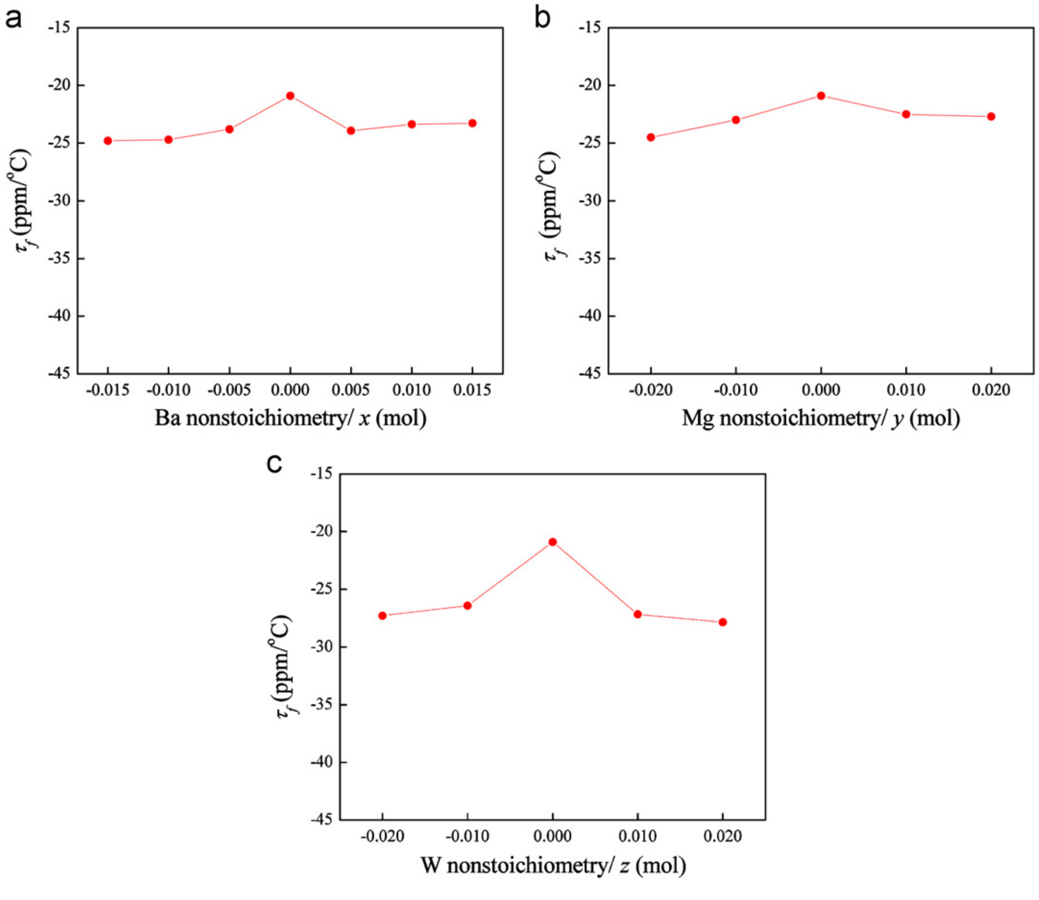

Fig. 10. Variation of τ_f with nonstoichiometry for (a) $Ba_{1+x}(MgW)_{1/2}O_3$, (b) $Ba(Mg_{1+y}W)_{1/2}O_3$ and (c) $Ba(MgW_{1+z})_{1/2}O_3$ ceramics.

ceramic have been investigated. Crystal structure such as B-site 1:1 ordering degree changed little with the nonstoichiometry. Evaporation of BaO was confirmed during the sintering of BMW ceramics, which in turn produce more $BaWO_4$ phase. Ba-deficiency or W-excess in BMW could improve the sinterability and $Q\times f$ value due to the increase in $BaWO_4$ liquid phase and decrease in BaO lossy phase and porosity. Whereas Ba-excess or W-deficiency could suppress the formation of $BaWO_4$ at the expense of increase in sintering temperature and decrease in $Q\times f$ value. Mg nonstoichiometry (y) has little effect on the variation of $BaWO_4$ content due to the low vapor pressure at the sintering temperature. Maximum $Q\times f$ value of about 140,000 GHz could be obtained for the Ba-deficient or W-excessive samples after sintering at 1500 °C/2 h or 1550 °C/2 h, respectively. The $Q\times f$ value changes little for the Mg-nonstoichiometric compositions. All samples exhibit high $Q\times f$ value of about 120,000 GHz after sintering at 1550 °C/2 h. The influence of the MgO and $BaWO_4$ impurity phases on the dielectric permittivity can be neglected due to their comparatively high $Q\times f$ values and trace amounts. The optimized dielectric permittivity for the well-densified samples is about 19–20. The τ_f values for all compositions are within the range of -21–-28 ppm/°C.

Acknowledgments

The authors are thankful to Mr. Lu Bo for recording XRD patterns (Rigaku D\max 2200, Tokyo, Japan), Mr. Chu Yuliang for SEM (HITACHI SU-1500, Japan).

References

[1] H. Takahashi, K. Ayusawa, N. Sakamoto, Microwave dielectric properties of $Ba(Mg_{1/2}W_{1/2})O_3$–$BaTiO_3$ ceramics, Japanese Journal of Applied Physics 36 (1997) 5597–5599.

[2] D.D. Khalyvin, J. Han, A.M.R. Senos, P.Q. Mantas, Synthesis and dielectric properties of tungsten-based complex perovskites, Journal of Materials Research 2003 (1811) 2600–2607.

[3] F. Zhao, Z.X. Yue, Z.L. Gui, L.T. Li, Preparation, characterization and microwave dielectric properties of A_2BWO_6 (A = Sr, Ba; B = Co, Ni, Zn) double perovskite ceramics, Japanese Journal of Applied Physics 44 (2005) 8066–8070.

[4] J.J. Bian, K. Yan, Y.F. Dong, Microwave dielectric properties of $A_{1-3x/2}La_x(Mg_{1/2}W_{1/2})O_3$ (A = Ba, Sr, Ca; $0.0\leq x\leq 0.05$) double perovskites, Materials Science and Engineering B 147 (2008) 27–34.

[5] J.Y. Wu, J.J. Bian, Structure stability and microwave dielectric properties of double perovskite ceramics–$Ba_2Mg_{1-x}Ca_xWO_6$ ($0.0\leq x\leq 0.15$), Ceramics International 38 (2012) 3217–3225.

[6] L.L.Y. Chang, M.G. Scroger, B. Phillips, Alkaline-earth tungstates: equilibrium and stability in the M–W–O Systems, Journal of the American Ceramic Society 49 (7) (1966) 385–390.

[7] S.H. Yoon, D.W. Kim, S.Y. Cho, K.S. Hong, Investigation of the relations between structure and microwave dielectric properties of divalent metal tungstate compounds, Journal of the European Ceramic Society 26 (2006) 2051–2054.

[8] B. Jancarw, J. Bezjak, P.K. Davies, High-temperature decomposition of B-site-ordered perovskite $Ba(Zn_{1/2}W_{1/2})O_3$, Journal of the American Ceramic Society 93 (3) (2010) 758–764.

[9] R.H. Lamoreaux, D.L. Hildenbrand, L. Brewer, High temperature vaporization behavior of oxides II. Oxides of Be, Mg, Ca, Sr, Ba, B, Al, Ga, In, Tl, Si, Ge, Sn, Pb, Zn, Ca and Hg, Journal of Physical and Chemical Reference Data 163 (1997) 419–433.

[10] H. Wu, P.K. Davies, Influence of non-stoichiometry on the structure and properties of $Ba(Zn_{1/3}Nb_{2/3})O_3$ microwave dielectrics: II compositional variations in pure BZN, Journal of the American Ceramic Society 89 (7) (2006) 2250–2263.

[11] K.P. Surendran, M.T. Sebastian, P. Mohanan, R.L. Moreira, A. Dias, Effect of nonstoichiometry on the structure and microwave dielectric properties of $Ba(Mg_{0.33}Ta_{0.67})O_3$, Chemistry of Materials 17 (2005) 142–151.

[12] J.H. Paik, S. Nahm, J.D. Bylin, M.H. Kim, H.J. Lee, The effect of Mg deficiency on the microwave dielectric properties of $Ba(Mg_{1/3}Nb_{2/3})O_3$ ceramics, Journal of Materials Science Letters 17 (1998) 1777–1780.

[13] J.J. Bian, G.X. Song, K. Yan, Structure and microwave dielectric properties of $Ba_{1+x}[(Co_{0.7}Zn_{0.3})_{1/3}Nb_{2/3}]O_3$ ($-0.015\leq x\leq 0.015$), Journal of the European Ceramic Society 27 (2007) 2817–2821.

[14] Q. Guo, O. Jakob, Enthalpies of formation from the component oxides of $MgWO_4$, $CaWO_4$ (scheelite), $SrWO_4$, and $BaWO_4$, determined by high-temperature direct synthesis calorimetry, Thermochimica Acta 288 (1996) 53–61.

[15] D.A. Durilin, O.V. Ovchar, A.G. Belous, Effect of nonstoichiometry on the structure and microwave dielectric properties of $Ba_{1-x}(Zn_{1/2}W_{1/2})O_{3-x}$ and $Ba(Zn_{1/2-y}W_{1/2})O_{3-y/2}$, Inorganic Materials 3 (47) (2011) 313–316.

[16] A. Kan, H. Ogawa, M. Sumino, M. Nishizuka, E. Suzuki, Microwave dielectric properties of xMgO-$(1-x)B_2O_3$ ceramics, Japanese Journal of Applied Physics 48 (2009) 5 09KE03.